

PREPARED FOR THE U.S. DEPARTMENT OF ENERGY,
UNDER CONTRACT DE-AC02-76CH03073

PPPL-3934
UC-70

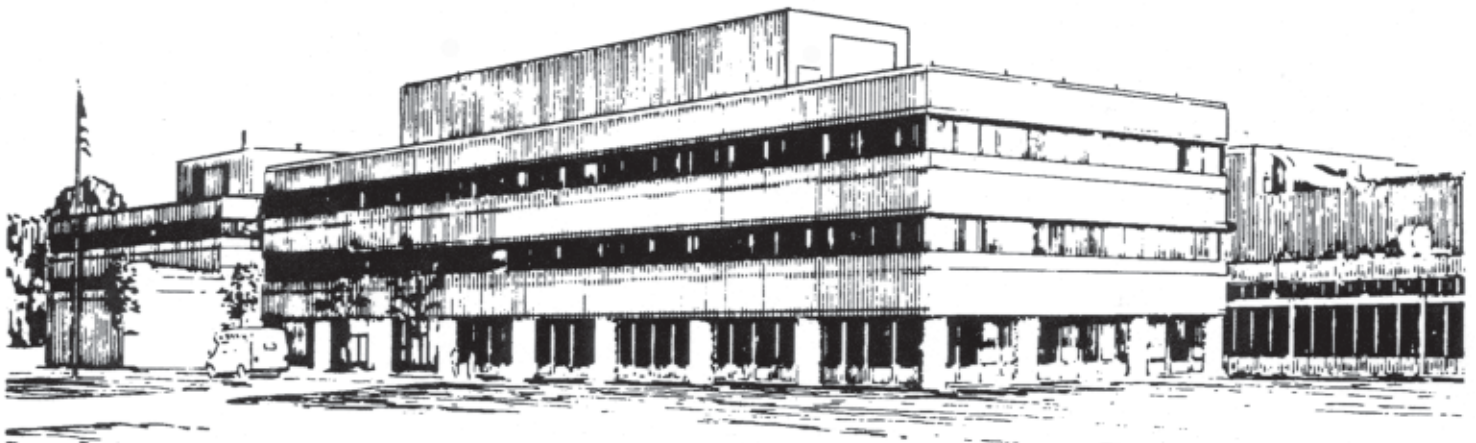
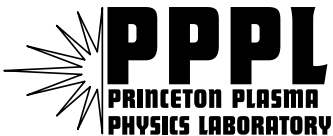
PPPL-3934

**Trapped Electron Stabilization of Ballooning Modes
in Low Aspect Ratio Toroidal Plasmas**

by

C.Z. Cheng and N.N. Gorelenkov

March 2004



**PRINCETON PLASMA PHYSICS LABORATORY
PRINCETON UNIVERSITY, PRINCETON, NEW JERSEY**

PPPL Reports Disclaimer

This report was prepared as an account of work sponsored by an agency of the United States Government. Neither the United States Government nor any agency thereof, nor any of their employees, makes any warranty, express or implied, or assumes any legal liability or responsibility for the accuracy, completeness, or usefulness of any information, apparatus, product, or process disclosed, or represents that its use would not infringe privately owned rights. Reference herein to any specific commercial product, process, or service by trade name, trademark, manufacturer, or otherwise, does not necessarily constitute or imply its endorsement, recommendation, or favoring by the United States Government or any agency thereof. The views and opinions of authors expressed herein do not necessarily state or reflect those of the United States Government or any agency thereof.

Availability

This report is posted on the U.S. Department of Energy's Princeton Plasma Physics Laboratory Publications and Reports web site in Fiscal Year 2004. The home page for PPPL Reports and Publications is: http://www.pppl.gov/pub_report/

DOE and DOE Contractors can obtain copies of this report from:

U.S. Department of Energy
Office of Scientific and Technical Information
DOE Technical Information Services (DTIS)
P.O. Box 62
Oak Ridge, TN 37831

Telephone: (865) 576-8401

Fax: (865) 576-5728

Email: reports@adonis.osti.gov

This report is available to the general public from:

National Technical Information Service
U.S. Department of Commerce
5285 Port Royal Road
Springfield, VA 22161

Telephone: 1-800-553-6847 or
(703) 605-6000

Fax: (703) 321-8547

Internet: <http://www.ntis.gov/ordering.htm>

Trapped Electron Stabilization of Ballooning Modes in Low Aspect Ratio Toroidal Plasmas

C. Z. Cheng and N. N. Gorelenkov

Princeton Plasma Physics Laboratory, Princeton University,

Princeton, NJ 08543

(March 15, 2004)

The kinetic effects of trapped electron dynamics and finite gyroradii and magnetic drift motion of ions are shown to give rise to a large parallel electric field and hence a parallel current that greatly enhances the stabilizing effect of field line tension for ballooning modes in low aspect ratio toroidal plasmas. For large aspect ratio the stabilizing effect increases (reduces) the $\beta(= 2P/B^2)$ threshold for the first (second) stability of the kinetic ballooning mode (KBM) from the MHD β threshold value by a factor proportional to the trapped electron density fraction. For small aspect ratio the stabilizing effect can greatly increase the β threshold of the first stability of KBMs from the MHD β threshold by $S_c \simeq 1 + (n_e/n_{eu})\delta$, where n_e/n_{eu} is the ratio of the total electron density to the untrapped electron density, and δ depends on the trapped electron dynamics and finite gyroradii and magnetic drift motion of ions. If $n_e/n_{eu} \gg 1$ as in the National Spherical Torus Experiment (NSTX) with an aspect ratio of $\simeq 1.4$, the KBM should be stable for $\beta \leq 1$ for finite magnetic shear. Therefore, unstable KBMs are expected only in the weak shear region near the radial location of the minimum of the safety factor in NSTX reverse shear discharges.

I. INTRODUCTION

One of the most serious instabilities in magnetically confined nonuniform plasmas is the ballooning instability which results from the release of free energy of nonuniform pressure with a gradient in the same direction as the magnetic field curvature. Analogous to the expansion of a balloon due to higher inner air pressure around weak surface tension spot, the ballooning instability will relax higher plasma pressure and hence move the plasma across the magnetic field lines toward the weaker pressure direction around the weak field line tension region as a result of the plasma frozen-in condition. In this paper we present a kinetic theory of ballooning instability which shows that the kinetic effects of trapped electron dynamics, finite Larmor radii (FLR) and magnetic drift motion of ions, and wave-particle resonances are important in determining the stability of ballooning modes. In particular, we show that the combined kinetic effects of trapped electron dynamics and ion motion perpendicular to the field line (finite Larmor radii and magnetic drift motion) give rise to a large parallel electric field and hence a parallel current that greatly enhances the stabilizing effect of field line tension. For large aspect ratio with $R_0/r \gg 1$, where R_0 is the major radius and r is the minor radius, the stabilizing effect increases (reduces) the $\beta (= 2P/B^2)$ threshold for the first (second) stability of the kinetic ballooning mode (KBM) from the MHD β threshold value by a factor proportional to the trapped electron density fraction ($\sim \sqrt{2r/R_0}$). For low aspect ratio ($R_0/r \sim 1$) such as in the National Spherical Torus Experiment (NSTX), we expect the total electron density to be much larger than the untrapped electron density ($n_e/n_{eu} \simeq 1/[1 - \sqrt{2r/(R_0 + r)}] \gg 1$) and the stabilizing kinetic effects increase the critical β of the first KBM stability over the MHD prediction by a factor proportional to n_e/n_{eu} .

Most studies of the ballooning instability have been based on the ideal MHD model. The fundamental shortcomings of the MHD model are: (a) based on the Ohm's law the plasma is assumed to be frozen in the field lines and moves across the field with a $\mathbf{E} \times \mathbf{B}$ drift velocity and the parallel electric field vanishes; (b) the plasma pressure changes adiabatically according to the adiabatic pressure law; and (c) the gyro-viscous tensor that contains finite particle

Larmor radius effects is ignored in the momentum equation. The Ohm's law and adiabatic pressure law are appropriate only if the frequency, ω , and perturbation wavenumber, \mathbf{k} , satisfy the ordering assumptions that $\omega_{ci} \gg \omega \gg \omega_b, \omega_d$ for both electrons and ions and $L > k^{-1} \gg \rho_i$, where ω_{ci} is the ion cyclotron frequency, ω_b is the particle bounce frequency, ω_d is the particle magnetic (∇B and curvature) drift frequency, L is the background plasma and magnetic field scale length, and ρ_i is the ion Larmor radius. These assumptions can easily break down for many critical plasma phenomena.

We shall consider the phase speed of KBMS along the field line to be much smaller than the electron thermal speed, but much larger than the ion thermal speed. This condition is satisfied for collisionless high temperature plasmas in most laboratory fusion devices because the frequency of ballooning modes is on the order of the ion diamagnetic drift frequency and the temperatures of electrons and ions are of the same order. Therefore, with respect to the wave motion along the ambient magnetic field lines electrons move very rapidly with either transit or bounce motion depending on the particle pitch angle. On the other hand, ions moves very slowly with respect to the parallel wave motion and their parallel dynamics can be considered as static. Moreover, electron and ion motions across the magnetic field lines are very different if the perpendicular wavelength is on the order of ion gyroradii; the electron perpendicular motion is essentially the combination of $\mathbf{E} \times \mathbf{B}$ and magnetic drift motion because of small gyroradii, but the ion perpendicular motion is governed by the $\mathbf{E} \times \mathbf{B}$, magnetic drifts as well as the polarization drift due to finite gyroradii. The difference in electron and ion motion across magnetic field lines causes charge separation. In order to maintain the charge quasi-neutrality a parallel electric field must be produced to accelerate (or decelerate) electrons to positions where there is excess positive charge. A parallel electric field can easily accelerate (or decelerate) untrapped electrons to change its density distribution. However, it is relatively harder to change the trapped electron density distribution by a parallel electric field because of their rapid bounce motion along the field lines. Thus, a parallel electric field enhanced by a factor of $1 + O(n_e/n_{eu})$, where n_e and n_{eu} are the total electron density and the untrapped electron density respectively,

will be produced to move the untrapped electrons to maintain charge quasi-neutrality. The large parallel electric field will then drive an enhanced parallel current which can greatly increase the stabilizing field line tension over the value expected from the MHD theory just like the high-pressured water in a hose increases the tension of the hose. For large aspect ratio with $\varepsilon = r/R_0 \ll 1$, the fraction of trapped electron population is much smaller than the untrapped fraction and $n_e/n_{eu} \sim 1 + O(\sqrt{\varepsilon})$, and the critical β (β_c) for the first (second) kinetic ballooning stability is larger (smaller) than the ideal MHD threshold β_c^{MHD} by a factor proportional to $\sqrt{\varepsilon}$. For small aspect ratio with $r/R_0 \sim O(1)$, the fraction of trapped electron population is much larger than the untrapped fraction and $n_{eu}/n_e \simeq 1 - \text{sqr}t1 - (R_0 - r)/(R_0 + r) \simeq (R_0 - r)/2(R_0 + r) \ll 1$. Then, the first stability β_c of the kinetic ballooning mode is enhanced over β_c^{MHD} by $O(n_e/n_{eu})$. For an aspect ratio of $R_0/r = 1.5$ as in NSTX, β_c can be a factor of $n_{eu}/n_e \simeq 10$ larger than β_c^{MHD} and we expect the KBM to be stable in the finite magnetic shear region. However, if NSTX has a reverse shear, then the KBM is expected to be unstable around the radial location of the minimum safety factor, where the magnetic shear is very weak.

KINETIC EIGENMODE EQUATIONS

To properly address kinetic effects on the ballooning instability we will employ the gyrokinetic formulation [1] to describe the particle dynamics. We shall consider collisionless plasmas with isotropic pressure. The particle velocity distribution function is assumed to have no appreciable bulk drift. Quasi-static equilibria with isotropic pressure are determined by the system of equations in the rationalized MKS unit: $\mathbf{J} \times \mathbf{B} = \nabla P$, $\nabla \times \mathbf{B} = \mathbf{J}$, and $\nabla \cdot \mathbf{B} = 0$. Assuming that the three-dimensional equilibrium has nested magnetic surfaces, the magnetic field can be expressed in a straight field line (ψ, α, θ) flux coordinate as $\mathbf{B} = \nabla\psi \times \nabla\alpha$, where ψ is the magnetic flux function, $\alpha = \zeta - q(\psi)\theta$, θ is a generalized poloidal angle, $\zeta = \phi - \delta(\psi, \phi, \theta)$ is a generalized toroidal angle, ϕ is the azimuthal angle in the cylindrical (R, ϕ, Z) coordinate, $q(\psi)$ is the safety factor, and $\delta(\psi, \phi, \theta)$ is periodic in

both ϕ and θ . The intersection of constant ψ and α surfaces defines the magnetic field line. The flux coordinate system is in general not orthogonal, and $\nabla\psi \cdot \nabla\theta \neq 0$, $\nabla\psi \cdot \nabla\alpha \neq 0$, and $\nabla\alpha \cdot \nabla\theta \neq 0$. Note that α is a cyclic function with a period of 2π for all constant ψ surfaces.

We consider low frequency perturbations with $\omega \ll \omega_{ci}$ and $k_{\perp}L \gg k_{\parallel}L > 1$, where ω is the wave frequency, ω_{ci} is the ion cyclotron frequency, L is the equilibrium scale length, and \parallel and \perp denotes the parallel and perpendicular component to the ambient magnetic field \mathbf{B} , respectively. Because the electron mass is much smaller than the ion mass and the temperatures of electrons and ions are of the same order, the electron thermal velocity is much larger than the ion thermal velocity. We consider electromagnetic perturbations with the orderings: $k_{\perp}\rho_i \sim O(1)$ and $v_{the} > (\omega/k_{\parallel}) > v_{thi}$ [2,3], where ρ_i is the ion gyroradius. With these orderings the following kinetic effects must be considered: trapped electron dynamics, ion FLR effect and wave-particle resonance with $\omega - \omega_{di} = 0$, where ω_{di} is the ion magnetic drift frequency. We shall obtain approximate solutions of the perturbed particle distributions based on the gyrokinetic formulation [6].

For $k_{\perp} \gg k_{\parallel}$ we assume a WKB representation for perturbed quantities, *i.e.*, $\delta f(\mathbf{x}, \mathbf{v}, t) = \delta f(s, \mathbf{k}_{\perp}, \mathbf{v}) \exp[i(S - \omega t)]$, where s is the distance along a field line, $\mathbf{k}_{\perp} = \nabla S$, S is the WKB eikonal. Including full FLR effects the perturbed particle distribution function for species j can be expressed in terms of the rationalized MKS unit as

$$\delta f(s, \mathbf{k}_{\perp}, \mathbf{v}) = \frac{q}{m} \frac{\partial F}{\partial \mathcal{E}} \left[\frac{\omega_{\star}^T}{\omega} + \left(1 - \frac{\omega_{\star}^T}{\omega} \right) \left(1 - J_0 e^{i\delta L} \right) \right] \Phi + g e^{i\delta L}, \quad (1)$$

where the j subscript has been omitted, q is the particle charge, m is the particle mass, B is the magnetic field intensity, $\mathcal{E} = v^2/2$, the guiding center particle equilibrium distribution is assumed to be $F = F(\mathcal{E}, \psi)$ so that the equilibrium pressure is a function of \mathcal{E} and ψ only, $\omega_{\star}^T = \mathbf{B} \times \mathbf{k}_{\perp} \cdot \nabla F / (\omega_c B \partial F / \partial \mathcal{E})$, $\omega_c = qB/m$ is the cyclotron frequency, $\delta L = \mathbf{k}_{\perp} \times \mathbf{v} \cdot \mathbf{B} / \omega_c B$, J_l is the l -th order Bessel function of the argument $k_{\perp} v_{\perp} / \omega_c$, Φ is the perturbed electrostatic potential, and g is the nonadiabatic part of the perturbed distribution function. Note that the subscript for particle species has been neglected. Based on the WKB

formalism the gyrokinetic equation for g in the low frequency ($\omega \ll \omega_c$) limit is given by

$$(\omega - \omega_d + i\mathbf{v}_{\parallel} \cdot \nabla_{\parallel})g = -\frac{q}{m} \frac{\partial F}{\partial \mathcal{E}} \left(1 - \frac{\omega_{*}^T}{\omega}\right) \left[(\omega_d \Phi - i\mathbf{v}_{\parallel} \cdot \nabla_{\parallel} \Psi) J_0 + \frac{\omega v_{\perp}}{k_{\perp}} J_1 \delta B_{\parallel} \right], \quad (2)$$

where Ψ is the parallel perturbed electric field potential with $\mathbf{E}_{\parallel} = -\nabla_{\parallel} \Psi$, δB_{\parallel} is the perturbed parallel magnetic field, $\omega_d = \mathbf{k}_{\perp} \cdot \mathbf{v}_d$ is the magnetic drift frequency, $\mathbf{v}_d = (m\mathbf{B}/qB^2) \times (v_{\parallel}^2 \boldsymbol{\kappa} + \mu \nabla B)$ is the magnetic drift velocity, $\boldsymbol{\kappa} = (\mathbf{B}/B) \cdot \nabla (\mathbf{B}/B)$ is the magnetic field curvature, and $\mu = v_{\perp}^2/2B$ is the magnetic moment. Note that the vector potential, defined by $\mathbf{A} = \mathbf{A}_{\parallel} + A_{\perp} \mathbf{B} \times \mathbf{k}_{\perp}/(Bk_{\perp})$, is related to Φ , Ψ and δB_{\parallel} by $\omega \mathbf{A}_{\parallel} = -i\nabla_{\parallel}(\Phi - \Psi)$ and $\delta B_{\parallel} = ik_{\perp} A_{\perp}$.

In the following we will derive three coupled equations from perpendicular and parallel Ampere's law and quasineutrality condition for three unknowns, Φ , Ψ and δB_{\parallel} . The derivation is based on the solution of Eq.(2) for ions and electrons with Maxwellian equilibrium distribution functions with temperature T . To obtain the perturbed ion distribution function we assume that $\omega, \omega_{di} \gg |v_{\parallel} \nabla_{\parallel}|$, and thus the ion dynamics is mainly determined by its perpendicular motion, and the nonadiabatic perturbed ion distribution function is given by

$$g_i \simeq \frac{q_i F_i}{T_i} \frac{\omega - \omega_{*i}^T}{\omega - \omega_{di}} \left(\frac{\omega_{di}}{\omega} J_0 \Phi + \frac{v_{\perp}}{k_{\perp}} J_1 \delta B_{\parallel} \right), \quad (3)$$

where the subscript i refers to the ion species. Note that the ion dynamics is mainly determined by its perpendicular motion.

For electrons we shall neglect FLR effects and consider $|v_{\parallel} \nabla_{\parallel}| \gg \omega, \omega_{de}$. Clearly, trapped and un-trapped electrons have very different parallel dynamics. The un-trapped electron dynamics is mainly determined by its fast parallel transit motion, and to the lowest order in $(\omega/|v_{\parallel} \nabla_{\parallel}|)$ the perturbed un-trapped electron distribution function is given by

$$g_{eu} \simeq -\frac{q_e F_e}{T_e} \left(1 - \frac{\omega_{*e}^T}{\omega}\right) \Psi. \quad (4)$$

where the subscript e refers to the electrons. The trapped electron dynamics is mainly determined by its fast parallel bounce motion. We perform the bounce averaging of Eq.(2) and to the lowest order in (ω/ω_{be}) we obtain

$$g_{et} \simeq \frac{q_e F_e}{T_e} \left\{ \left(\frac{\omega_{*e}^T}{\omega} - 1 \right) \left(\Psi - \frac{\langle (\omega - \omega_{de}) \Psi \rangle}{\omega - \langle \omega_{de} \rangle} \right) + \frac{\omega - \omega_{*e}^T}{\omega - \langle \omega_{de} \rangle} \left\langle \frac{\omega_{de}}{\omega} \Phi + \frac{m_e v_{\perp}^2}{2q_e B} \delta B_{\parallel} \right\rangle \right\}, \quad (5)$$

where $\langle X \rangle = \oint ds X / v_{\parallel} / \oint ds / v_{\parallel}$ is the trapped particle orbit average of X and is a function of particle pitch angle. The magnetic drift frequencies for ions and electrons are given by

$$\omega_{dj} = \frac{m_j \mathcal{E}}{T_j} \left\{ \hat{\omega}_{kj} \left(1 - \frac{\mu B}{2\mathcal{E}} \right) - \omega_{*j} \frac{\mu B}{2\mathcal{E}} [\beta_e (1 + \eta_e) + \beta_i (1 + \eta_i)] \right\}, \quad (6)$$

where we make use $\omega_{*j} [\beta_e (1 + \eta_e) + \beta_i (1 + \eta_i)] + \hat{\omega}_{Bj} = \hat{\omega}_{kj}$ from the equilibrium relation $\nabla_{\perp} (P + B^2/2) = \kappa B^2$, $\beta_e = 2n_e T_e / B^2$, $\beta_i = 2n_i T_i / B^2$, $\eta_e = d \ln T_e / d \ln n_e$, $\eta_i = d \ln T_i / d \ln n_i$, $\hat{\omega}_{Bj} = 2\mathbf{B} \times \nabla B \cdot \mathbf{k}_{\perp} T_j / q_j B^3$, $\hat{\omega}_{kj} = 2\mathbf{B} \times \kappa \cdot \mathbf{k}_{\perp} T_j / q_j B^2$, and $\omega_{*j} = \mathbf{B} \times \nabla \ln n_j \cdot \mathbf{k}_{\perp} T_j / q_j B^2$.

Substituting the perturbed distribution functions for all particle species into the quasineutrality condition, $\sum_j \int q_j f_j d^3 v = 0$, where the summation over j is over all particle species, we obtain:

$$- \int d^3 v \frac{q_i^2}{m_i} \frac{\partial F_i}{\partial \mathcal{E}} \left(1 - \frac{\omega_{*i}^T}{\omega} \right) (1 - J_0^2) \Phi = \sum_j q_j \int d^3 v J_0 g_j. \quad (7)$$

Using solutions of the drift kinetic equation, Eq.(7) is reduced to the following expression for the parallel electric field potential:

$$\begin{aligned} \left(\frac{n_{eu} + n_{et} \Delta_1}{n_e} \right) \left(1 - \frac{\omega_{*e}}{\omega} \right) \Psi = E_{1a} \Phi - \frac{n_i q_i^2 T_e}{n_e q_e^2 T_i} \left[\left(1 - \frac{\omega_{*pi}}{\omega} \right) (1 - \Gamma_0) + G - I_1 \right] \Phi \\ + \frac{T_e}{q_e B} E_{1b} \delta B_{\parallel} + \left(\frac{n_i q_i^2 T_e}{n_e q_e^2 T_i} \right) I_2 \frac{T_i}{q_i B} \delta B_{\parallel} \end{aligned} \quad (8)$$

where $n_{et}/n_e \equiv R_1 = \sqrt{1 - B/B_{\max}}$ and $n_{eu}/n_e = 1 - R_1$ are the fraction of trapped and passing (untrapped) electron densities, respectively, B_{\max} is the maximum magnetic field along a field line, Δ_1 is an operator involving trapped electron orbit average of the parallel electric potential Ψ and is given by

$$\Delta_1 \Psi = \int d^3 v \frac{F_{et}}{n_{et}} \left(\frac{\omega - \omega_{*e}^T}{\omega - \omega_{*e}} \right) \left[\Psi - \frac{\langle (\omega - \omega_{de}) \Psi \rangle}{\omega - \langle \omega_{de} \rangle} \right], \quad (9)$$

$G = (\eta_i \omega_{*i} / \omega) [(1 - \Gamma_0) - b_i (\Gamma_0 - \Gamma_1)]$, $\Gamma_{0,1}(b_i) = I_{0,1}(b_i) \exp(-b_i)$, $b_i = k_{\perp}^2 T_i / m_i \omega_{ci}^2 = k_{\perp}^2 \rho_i^2 / 2$, I_0 and I_1 are the modified Bessel function of the zeroth order and first order, respectively, $\omega_{*pj} = \omega_{*j} (1 + \eta_j)$, $\eta_j = \nabla \ln T_j / \nabla \ln n_j$,

$$I_1 = \int d^3v \frac{F_i \omega - \omega_{*i}^T \omega_{di}}{n_i \omega - \omega_{di}} \frac{J_0^2}{\omega}, \quad (10)$$

$$I_2 = \int d^3v \frac{F_i \omega - \omega_{*i}^T q_i B v_\perp}{n_i \omega - \omega_{di}} \frac{J_0 J_1}{T_1 k_\perp}, \quad (11)$$

and E_{1a} and E_{1b} are operators involving trapped electron orbit average of perturbed variables and are given by

$$E_{1a} \Phi = \int d^3v \frac{F_{et} \omega - \omega_{*e}^T \langle \omega_{de} \Phi \rangle}{n_e \omega - \langle \omega_{de} \rangle} \frac{1}{\omega}, \quad (12)$$

and

$$E_{1b} \delta B_\parallel = \int d^3v \frac{F_{et} \omega - \omega_{*e}^T m_e v_\perp^2}{n_e \omega - \langle \omega_{de} \rangle} \frac{1}{2T_e} \langle \delta B_\parallel \rangle. \quad (13)$$

We can express the electron bounce-averaged magnetic drift frequency as $\omega_{de} = \hat{\omega}_{de} m_e \mathcal{E} / T_e \equiv \hat{\omega}_{de} \hat{v}^2$, where $\hat{\omega}_{de}$ is a function of particle pitch angle but not energy. Then, $E_{1a} \Phi$ can be integrated over the particle energy and is given by

$$E_{1a} \Phi = \int_{h_m}^h \frac{d\lambda}{2h\sqrt{1-\lambda/h}} \hat{E}_1 \frac{\langle \hat{\omega}_{de} \Phi \rangle}{\langle \hat{\omega}_{de} \rangle}, \quad (14)$$

where $\int d^3v = \sum_\sigma \pi \int_0^\infty dv v^2 \int_0^h d\lambda / (h\sqrt{1-\lambda/h})$, $\lambda = \mu B_0 / \mathcal{E}$, $h = B_0 / B$, the sum σ accounts for two directions of particle motion along the field line, B_0 is a reference magnetic field intensity that can be chosen arbitrarily, $h_m = B_0 / B_{max}$ and

$$\begin{aligned} \hat{E}_1 &\equiv \frac{4}{\sqrt{\pi}} \int_0^\infty d\hat{v} \hat{v}^4 e^{-\hat{v}^2} \frac{\omega - \omega_{*e}^T \langle \hat{\omega}_{de} \rangle}{\omega - \langle \omega_{de} \rangle} \frac{1}{\omega} \\ &= \frac{3\eta_e \omega_{*e}}{2\omega} - \left\{ 1 - \frac{\omega_{*e}}{\omega} \left[1 + \eta_e \left(\xi_e^2 - \frac{3}{2} \right) \right] \right\} \left[1 + 2\xi_e^2 (1 + \xi_e Z(\xi_e)) \right], \end{aligned} \quad (15)$$

where $Z(\xi_e) = \pi^{-1/2} \int_{-\infty}^\infty e^{-t^2} (t - \xi_e)^{-1} dt$ is the plasma dispersion function, and $\xi_e^2 = \omega / \langle \hat{\omega}_{de} \rangle$. Similarly, $E_{1b} \delta B_\parallel$ is reduced to

$$E_{1b} \delta B_\parallel = \int_{h_m}^h \frac{d\lambda}{2h\sqrt{1-\lambda/h}} \left(\frac{\lambda}{h} \right) \frac{\omega}{\langle \hat{\omega}_{de} \rangle} \hat{E}_1 \langle \delta B_\parallel \rangle. \quad (16)$$

I_1 , and I_2 can also be integrated over v_\parallel and they are given by

$$I_1 = \frac{\omega}{\hat{\omega}_{ki}} \int_0^\infty dx e^{-x} J_0^2 \left\{ \left(\frac{-Z(\xi_i)}{\xi_i} \right) \left[1 - \frac{\omega_{*i}}{\omega} \left(1 - \eta_i \left(\frac{3}{2} - x - \xi_i^2 \right) \right) \right] + \eta_i \frac{\omega_{*i}}{\omega} \right\} - \left[\left(1 - \frac{\omega_{*i}}{\omega} \right) \Gamma_0 + \frac{\eta_i \omega_{*i}}{\omega} b_i (\Gamma_0 - \Gamma_1) \right], \quad (17)$$

and

$$I_2 = \frac{\omega}{\hat{\omega}_{ki}} \int_0^\infty dx e^{-x} J_0 (J_0 + J_2) x \left\{ \left(\frac{-Z(\xi_i)}{\xi_i} \right) \left[1 - \frac{\omega_{*i}}{\omega} \left(1 - \eta_i \left(\frac{3}{2} - x - \xi_i^2 \right) \right) \right] + \eta_i \frac{\omega_{*i}}{\omega} \right\}, \quad (18)$$

where $\xi_i^2 = (\omega - \hat{\omega}_{Bi}x/2)/\hat{\omega}_{ki}$, and the argument of the Bessel functions is $(b_i x)^{1/2}$.

To obtain an equation for δB_{\parallel} , we employ the perpendicular component of the Ampere's law, $\nabla \times \delta \mathbf{B} = \delta \mathbf{J}$, which relates the perturbed magnetic field with the perturbed current, where $\delta \mathbf{J}$ is the perturbed current density. Using Eq.(1) we can write

$$\delta B_{\parallel} = - \sum_j q_j \int d^3 v \frac{v_{\perp}}{k_{\perp}} J_1 \left[g_j - \frac{q_j}{m_j} \frac{\partial F_j}{\partial \mathcal{E}} \left(1 - \frac{\omega_{*j}^T}{\omega} \right) J_0 \Phi \right]. \quad (19)$$

Using the solutions of the gyrokinetic equations, we obtain

$$\left(1 + \frac{\beta_i}{2} I_3 \right) \delta B_{\parallel} + \frac{\beta_e}{2} \xi_e^2 E_{2b} \delta B_{\parallel} = \frac{q_e B}{2T_e} \beta_e \left\{ \left(\frac{\omega_{*pe}}{\omega} - 1 - E_{2a} + I_2 \right) \Phi + \left(1 - \frac{3R_2}{2} \right) \left(1 - \frac{\omega_{*pe}}{\omega} \right) \Psi + \Delta_2 \Psi \right\}, \quad (20)$$

where $R_2 = 2R_1 (1 + B/2B_{\max})/3$,

$$I_3 = \int d^3 v \frac{F_i}{n_i} \frac{\omega - \omega_{*i}^T}{\omega - \omega_{di}} \left(\frac{q_i B v_{\perp}}{T_i k_{\perp}} \right)^2 J_1^2, \quad (21)$$

E_{2a} and E_{2b} , and Δ_2 are operators involving trapped electron orbit average of perturbed variables and are given by

$$E_{2a} \Phi = \int d^3 v \frac{F_{et}}{n_e} \left(\frac{m_e v_{\perp}^2}{2T_e} \right) \frac{\omega - \omega_{*e}^T}{\omega - \langle \omega_{de} \rangle} \frac{\langle \omega_{de} \Phi \rangle}{\omega}, \quad (22)$$

$$E_{2b} \delta B_{\parallel} = \int d^3 v \frac{F_{et}}{n_e} \left(\frac{m_e v_{\perp}^2}{2T_e} \right)^2 \frac{\omega - \omega_{*e}^T}{\omega - \langle \omega_{de} \rangle} \frac{\langle \hat{\omega}_{de} \rangle}{\omega} \langle \delta B_{\parallel} \rangle. \quad (23)$$

and

$$\Delta_2 \Psi = \int d^3 v \frac{F_{et}}{n_{et}} \left(\frac{m_e v_{\perp}^2}{2T_e} \right) \left(1 - \frac{\omega_{*e}^T}{\omega} \right) \left[\Psi - \frac{\langle (\omega - \omega_{de}) \Psi \rangle}{\omega - \langle \omega_{de} \rangle} \right]. \quad (24)$$

Again, integrating over the particle parallel velocity can be carried for I_3 and integrating over the particle energy can be performed in E_{2a} and E_{2b} , we have

$$I_3 = \frac{\omega}{\hat{\omega}_{ki}} \int_0^\infty dx e^{-x} (J_0 + J_2)^2 x^2 \left\{ \left(\frac{-Z(\xi_i)}{\xi_i} \right) \left[1 - \frac{\omega_{*i}}{\omega} \left(1 - \eta_i \left(\frac{3}{2} - x - \xi_i^2 \right) \right) \right] + \eta_i \frac{\omega_{*i}}{\omega} \right\}, \quad (25)$$

$$E_{2a}\Phi = \int_{h_m}^h \frac{d\lambda}{2h\sqrt{1-\lambda/h}} \left(\frac{\lambda}{h} \right) \hat{E}_2 \frac{\langle \hat{\omega}_{de}\Phi \rangle}{\langle \hat{\omega}_{de} \rangle}, \quad (26)$$

$$E_{2b}\delta B_{\parallel} = \int_{h_m}^h \frac{d\lambda}{2h\sqrt{1-\lambda/h}} \left(\frac{\lambda}{h} \right)^2 \hat{E}_2 \langle \delta B_{\parallel} \rangle, \quad (27)$$

where

$$\begin{aligned} \hat{E}_2 &\equiv \frac{4}{\sqrt{\pi}} \int_0^\infty d\hat{v} \hat{v}^6 e^{-\hat{v}^2} \frac{\omega - \omega_{*e}^T}{\omega - \langle \omega_{de} \rangle} \frac{\langle \hat{\omega}_{de} \rangle}{\omega} \\ &= \frac{15\eta_e \omega_{*e}}{4\omega} - \left\{ 1 - \frac{\omega_{*e}}{\omega} \left[1 + \eta_e \left(\xi_e^2 - \frac{3}{2} \right) \right] \right\} \left[\frac{3}{2} + \xi_e^2 + 2\xi_e^4 (1 + \xi_e Z(\xi_e)) \right], \end{aligned} \quad (28)$$

Finally, we obtain the vorticity equation to close the coupled equations for Φ , Ψ and δB_{\parallel} . By multiplying the gyrokinetic equation, Eq.(2), with particle charge, integrating over the velocity space, summing over all species, and making use of the parallel component of the Ampere's law which relates the perturbed parallel current to the perturbed field by $\delta J_{\parallel} \simeq -ik_{\perp}^2 \nabla_{\parallel} (\Phi - \Psi) / \omega$, we obtain the vorticity equation

$$\begin{aligned} \mathbf{B} \cdot \nabla \left(\frac{k_{\perp}^2}{B^2} \mathbf{B} \cdot \nabla (\Phi - \Psi) \right) - \omega^2 \sum_j \int d^3v \frac{q_j^2}{m_j} \frac{\partial F_j}{\partial \mathcal{E}} \left(1 - \frac{\omega_{*j}^T}{\omega} \right) \left[(1 - J_0^2) \Phi - \frac{v_{\perp}}{k_{\perp}} J_0 J_1 \delta B_{\parallel} \right] \\ - \omega \sum_j \int d^3v \omega_{dj} \left[q_j J_0 g_j - \frac{q_j^2}{m_j} \frac{\partial F_j}{\partial \mathcal{E}} \left(1 - \frac{\omega_{*j}^T}{\omega} \right) J_0^2 \Phi \right] = 0. \end{aligned} \quad (29)$$

Again, substituting the solutions from the gyrokinetic equations, the vorticity equation becomes

$$\begin{aligned} \frac{V_A^2 T_i}{m_i \omega_{ci}^2} \mathbf{B} \cdot \nabla \left(\frac{k_{\perp}^2}{B^2} \mathbf{B} \cdot \nabla (\Phi - \Psi) \right) + \omega^2 \left[\left(1 - \frac{\omega_{*pi}}{\omega} \right) (1 - \Gamma_0) + G - I_1 \right] \Phi \\ + \frac{q_e T_i}{q_i T_e} \left[(\omega - \omega_{*pe}) \left(\frac{\hat{\omega}_{Be} + \hat{\omega}_{ke}}{2} \right) + \omega^2 E_{3a} \right] \Phi + \omega^2 \left(1 - \frac{\omega_{*pe}}{\omega} - I_2 - E_{3b} \right) \frac{T_i}{q_i B} \delta B_{\parallel} \\ - \frac{q_e T_i}{q_i T_e} \left\{ \frac{(\omega - \omega_{*pe})}{2} \left[\hat{\omega}_{Be} \left(1 - \frac{3R_2}{2} \right) + \hat{\omega}_{ke} (1 + 3(R_2 - R_1)) \right] + \omega^2 \Delta_3 \right\} \Psi = 0. \end{aligned} \quad (30)$$

where $V_A = B/(n_i m_i)^{1/2}$ is the Alfvén speed, E_{3a} , E_{3b} , and Δ_3 are operators involving trapped electron orbit average of perturbed variables and are given by

$$E_{3a}\Phi = \int d^3v \frac{F_{et}}{n_e} \frac{\omega - \omega_{*e}^T}{\omega - \langle \omega_{de} \rangle} \frac{\omega_{de}}{\omega} \frac{\langle \omega_{de} \Phi \rangle}{\omega}, \quad (31)$$

$$E_{3b}\delta B_{\parallel} = \int d^3v \frac{F_{et}}{n_e} \left(\frac{m_e v_{\perp}^2}{2T_e} \right) \frac{\omega - \omega_{*e}^T}{\omega - \langle \omega_{de} \rangle} \frac{\omega_{de}}{\omega} \langle \delta B_{\parallel} \rangle. \quad (32)$$

and

$$\Delta_3\Psi = \int d^3v \frac{F_{et}}{n_{et}} \frac{\omega_{de}}{\omega} \left(1 - \frac{\omega_{*e}^T}{\omega} \right) \left[\Psi - \frac{\langle (\omega - \omega_{de}) \Psi \rangle}{\omega - \langle \omega_{de} \rangle} \right]. \quad (33)$$

Again, we can integrate over the particle energy in $E_{3a}\Phi$, and $E_{3b}\delta B_{\parallel}$, and we have

$$E_{3a}\Phi = \int_{h_m}^h \frac{d\lambda}{2h\sqrt{1-\lambda/h}} \left(\frac{\hat{\omega}_{Be}(\lambda/2h) + \hat{\omega}_{ke}(1-\lambda/h)}{\omega} \right) \hat{E}_2 \frac{\langle \hat{\omega}_{de} \Phi \rangle}{\langle \hat{\omega}_{de} \rangle}, \quad (34)$$

$$E_{3b}\delta B_{\parallel} = \int_{h_m}^h \frac{d\lambda}{2h\sqrt{1-\lambda/h}} \left(\frac{\lambda}{h} \right) \left(\frac{\hat{\omega}_{Be}(\lambda/2h) + \hat{\omega}_{ke}(1-\lambda/h)}{\omega} \right) \frac{\omega}{\langle \hat{\omega}_{de} \rangle} \hat{E}_2 \langle \delta B_{\parallel} \rangle, \quad (35)$$

Equations (8), (20) and (30) constitute the WKB-ballooning equations for the stability of low frequency modes such as the kinetic ballooning modes. However, they are integro-differential equations and are difficult to solve. Thus, to gain understanding of the mode stability further approximations must be made to simplify these equations.

SIMPLIFIED KINETIC BALLOONING EQUATIONS

To simplify the numerical procedures for solving Equations (8), (20) and (30) numerically, we make further assumptions to eliminate the bounce-averaged quantities for symmetric modes by assuming that $\langle (\omega - \omega_{de}) \Psi \rangle \simeq (\omega - \langle \omega_{de} \rangle) \Psi$, $\langle \omega_{de} \Phi \rangle \simeq \langle \omega_{de} \rangle \Phi$, and $\langle \delta B_{\parallel} \rangle \simeq \delta B_{\parallel}$. Then, Equations (8), (20) and (30) reduce to a set of differential equations. Moreover, $\Delta_1\Psi \simeq \Delta_2\Psi \simeq \Delta_3\Psi \simeq 0$. If we further assume that $\langle \omega_{de} \rangle$ does not depend on the particle pitch angle, then the pitch angle integrations in E_{1a} , E_{1b} , E_{2a} , E_{2b} , E_{3a} , E_{3b} can be carried out and we have $E_{1a} = R_1 \hat{E}_1$, $E_{1b} = (\omega / \langle \hat{\omega}_{de} \rangle) R_2 \hat{E}_1$, $E_{2a} = R_2 \hat{E}_2$, $E_{2b} = R_3 \hat{E}_2$,

$E_{3a} = [R_2\hat{\omega}_{Be}/2\omega + (R_1 - R_2)\hat{\omega}_{ke}/\omega]\hat{E}_2$, and $E_{3b} = [R_3\hat{\omega}_{Be}/2\langle\hat{\omega}_{de}\rangle + (R_2 - R_3)\hat{\omega}_{ke}/\langle\hat{\omega}_{de}\rangle]\hat{E}_2$, where $R_3 = (8R_1/15)[1 + B/2B_{\max} + (3/8)(B/B_{\max})^2]$. Then, Eqns. (8), (20) and (30) are further reduced to

$$\begin{aligned} \frac{n_{eu}}{n_e} \left(1 - \frac{\omega_{*e}}{\omega}\right) \Psi &= \frac{q_i T_e}{q_e T_i} \left[\left(1 - \frac{\omega_{*pi}}{\omega}\right) (1 - \Gamma_0) + G - I_1 \right] \Phi + R_1 \hat{E}_1 \Phi \\ &+ \left(\frac{\omega}{\langle\hat{\omega}_{de}\rangle} R_2 \hat{E}_1 - I_2 \right) \frac{T_e}{q_e B} \delta B_{\parallel}, \end{aligned} \quad (36)$$

$$\begin{aligned} &\left(1 + \frac{1}{2}\beta_i I_3 + \frac{1}{2}\beta_e R_3 \hat{E}_2 \omega / \langle\hat{\omega}_{de}\rangle\right) \delta B_{\parallel} \\ &= \frac{q_e B}{2T_e} \beta_e \left\{ \left(\frac{\omega_{*pe}}{\omega} - 1 - R_2 \hat{E}_2 + I_2\right) \Phi + \left(1 - \frac{3R_2}{2}\right) \left(1 - \frac{\omega_{*pe}}{\omega}\right) \Psi \right\}, \end{aligned} \quad (37)$$

and

$$\begin{aligned} &\frac{V_A^2 T_i}{m_i \omega_{ci}^2} \mathbf{B} \cdot \nabla \left(\frac{k_{\perp}^2}{B^2} \mathbf{B} \cdot \nabla (\Phi - \Psi) \right) + \omega^2 \left[\left(1 - \frac{\omega_{*pi}}{\omega}\right) (1 - \Gamma_0) + G - I_1 \right] \Phi \\ &+ \frac{q_e T_i}{q_i T_e} \left\{ (\omega - \omega_{*pe}) \left(\frac{\hat{\omega}_{Be} + \hat{\omega}_{ke}}{2} \right) + \hat{E}_2 \omega \left(\hat{\omega}_{Be} \frac{R_2}{2} + \hat{\omega}_{ke} (R_1 - R_2) \right) \right\} \Phi \\ &+ \omega^2 \left[1 - \frac{\omega_{*pe}}{\omega} + \hat{E}_2 \left(\frac{\hat{\omega}_{Be}}{\langle\hat{\omega}_{de}\rangle} \frac{R_3}{2} + \frac{\hat{\omega}_{ke}}{\langle\hat{\omega}_{de}\rangle} (R_2 - R_3) \right) - I_2 \right] \frac{T_i}{q_i B} \delta B_{\parallel} \\ &- \frac{q_e T_i}{q_i T_e} (\omega - \omega_{*pe}) \left[\hat{\omega}_{Be} \left(\frac{2 - 3R_2}{4} \right) + \hat{\omega}_{ke} \left(\frac{1 + 3(R_2 - R_1)}{2} \right) \right] \Psi = 0. \end{aligned} \quad (38)$$

To examine the kinetic ballooning stability for NSTX, a low aspect ratio tokamak, we shall present numerical solutions of equations (36)-(38) for numerical NSTX equilibria.

ANALYTICAL THEORY OF KINETIC BALLOONING INSTABILITY

To obtain an analytical understanding of the combined effects of trapped electron dynamics and finite ion Larmor radii, we consider the limits: $\omega \sim \omega_* \gg \omega_d$ for both electrons and ions, small ion Larmor radii $k_{\perp} \rho_i \ll 1$, low plasma beta $\beta_i, \beta_e < 1$. Then, $1 - \Gamma_0 \simeq b_i$, and $G \simeq O(b_i^2)$ and the integrals, \hat{E}_1 , \hat{E}_2 , I_1 , I_2 , and I_3 , can be reduced to the leading order as $\hat{E}_1 = (3\langle\hat{\omega}_{de}\rangle/2\omega)(1 - \omega_{*pe}/\omega)$, $\hat{E}_2 = (15\langle\hat{\omega}_{de}\rangle/4\omega)[1 - (1 + 2\eta_e)\omega_{*e}/\omega]$, $I_1 = (1 - \omega_{*pi}/\omega)(\hat{\omega}_{Bi} + \hat{\omega}_{ki})/2\omega$, $I_2 = 1 - \omega_{*pi}/\omega$, and $I_3 = 2[1 - (1 + 2\eta_i)\omega_{*i}/\omega]$.

First, we consider the large aspect ratio limit, i.e., $\varepsilon \equiv a/R_0 \ll 1$, then to the leading order $R_1 = R_2 = R_3 \sim O(\sqrt{\varepsilon})$ which represents the trapped electron density fraction. Equation (36), which determines the parallel electric field potential, is then simplified to the lowest order to

$$\left(1 - \frac{\omega_{*e}}{\omega}\right) \Psi \simeq (1 + R_1) \frac{q_i T_e}{q_e T_i} \left(1 - \frac{\omega_{*pi}}{\omega}\right) \left[\left(b_i - \frac{\hat{\omega}_{Bi} + \hat{\omega}_{ki}}{2\omega} \right) \Phi - \frac{T_i}{q_i B} \delta B_{\parallel} \right] + \frac{3R_1}{2} \left(1 - \frac{\omega_{*pe}}{\omega}\right) \left(\frac{\langle \hat{\omega}_{de} \rangle}{\omega} \Phi + \frac{T_e}{q_e B} \delta B_{\parallel} \right). \quad (39)$$

Note that the right-hand side is due to the perturbed ion density resulting from effects of finite ion Larmor radii and magnetic drifts. The contribution to the parallel electric field term on the left-hand-side is mainly due to the perturbed untrapped electron density. This is because the trapped electron density is not changed by the parallel electric field due to their fast bounce motion relative to the parallel wave motion. In comparison with the limit without trapped electron effects, the parallel electric field is enhanced by n_e/n_{eu} . Similarly, Eq. (45), which determines the parallel perturbed magnetic field, is simplified to the lowest order to

$$\frac{T_e}{q_e B} \delta B_{\parallel} \simeq \frac{\beta_e}{2} \left\{ \left(\frac{\omega_{*pe} - \omega_{*pi}}{\omega} \right) \Phi + \left(1 - \frac{\omega_{*pe}}{\omega} \right) \Psi - \frac{3R_1}{2} \left[\frac{5\langle \hat{\omega}_{de} \rangle}{2\omega} \left(1 - \frac{(1 - 2\eta_e)\omega_{*e}}{\omega} \right) \Phi + \left(1 - \frac{\omega_{*pe}}{\omega} \right) \Psi \right] \right\}. \quad (40)$$

Note that this relation is equivalent to the perturbed total pressure balance relation, $\mathbf{B} \cdot \delta \mathbf{B} + \delta P_{\perp} \simeq 0$, which is derived from MHD equations for low frequency instabilities with $\omega \ll k_{\perp} V_A$ [4–6]. The vorticity equation, Eq. (38), is simplified to

$$\begin{aligned} & \frac{V_A^2 T_i}{m_i \omega_{ci}^2} \mathbf{B} \cdot \nabla \left(\frac{k_{\perp}^2}{B^2} \mathbf{B} \cdot \nabla (\Phi - \Psi) \right) + \left[\omega (\omega - \omega_{*pi}) b_i + (\omega_{*pi} - \omega_{*pe}) \left(\frac{\hat{\omega}_{Bi} + \hat{\omega}_{ki}}{2} \right) \right] \Phi \\ & - (\omega - \omega_{*pe}) \left(\frac{\hat{\omega}_{Bi} + \hat{\omega}_{ki}}{2} \right) \Psi + \omega (\omega_{*pi} - \omega_{*pe}) \frac{T_i}{q_i B} \delta B_{\parallel} \\ & + R_1 \omega^2 \left[\frac{15}{8} \frac{\langle \hat{\omega}_{de} \rangle}{\omega} \left(1 - \frac{(1 + 2\eta_e)\omega_{*e}}{\omega} \right) \left(\frac{\hat{\omega}_{Bi}}{\omega} \Phi + \frac{\hat{\omega}_{Be}}{\langle \hat{\omega}_{de} \rangle} \frac{T_i}{q_i B} \delta B_{\parallel} \right) + \frac{3}{4} (\omega - \omega_{*pe}) \hat{\omega}_{Bi} \Psi \right] \simeq 0. \end{aligned} \quad (41)$$

Next, we eliminate δB_{\parallel} from the above three equations and to the leading order in $O(R_1)$ Eq. (39) reduces to

$$\begin{aligned} \left(1 - \frac{\omega_{*e}}{\omega}\right) \Psi \simeq & (1 + R_1) \frac{q_i T_e}{q_e T_i} \left(1 - \frac{\omega_{*pi}}{\omega}\right) \left(b_i - \frac{\hat{\omega}_{ki}}{\omega}\right) \Phi \\ & + \frac{3R_1}{2} \left(1 - \frac{\omega_{*pe}}{\omega}\right) \left[\frac{\langle \hat{\omega}_{de} \rangle}{\omega} + \frac{\beta_e (\omega_{*pe} - \omega_{*pi})}{2\omega}\right] \Phi, \end{aligned} \quad (42)$$

where we have made use of the equilibrium relation, $\beta_i(\omega_{*pi} - \omega_{*pe}) + \hat{\omega}_{Bi} = \hat{\omega}_{ki}$, which is equivalent to the equilibrium relation $\nabla_{\perp}(P + B^2/2) = \boldsymbol{\kappa}B^2$. Similarly, Eq. (41) reduces to

$$\begin{aligned} \frac{V_A^2 T_i}{m_i \omega_{ci}^2} \mathbf{B} \cdot \nabla \left(\frac{k_{\perp}^2}{B^2} \mathbf{B} \cdot \nabla (\Phi - \Psi) \right) + \omega (\omega - \omega_{*pi}) b_i \Phi + (\omega_{*pi} - \omega_{*pe}) \hat{\omega}_{ki} \Phi \\ + \frac{15R_1}{8} \left[\hat{\omega}_{ki} \langle \hat{\omega}_{de} \rangle + \frac{\beta_e}{2} \hat{\omega}_{Bi} (\omega_{*pe} - \omega_{*pi}) \right] \left(1 - \frac{(1 + 2\eta_e)\omega_{*e}}{\omega} \right) \Phi \\ - \left(1 - \frac{3R_1}{4} \right) (\omega - \omega_{*pe}) \hat{\omega}_{ki} \Psi \simeq 0, \end{aligned} \quad (43)$$

where we have made use of the relations: $-(\omega - \omega_{*pi})(\hat{\omega}_{Bi} + \hat{\omega}_{ki}) + (q_e T_i / q_i T_e)(\omega - \omega_{*pe})(\hat{\omega}_{ke} + \hat{\omega}_{Be}) - (q_e T_i / q_i T_e)(\omega_{*pi} - \omega_{*pe})^2 \beta_e = 2(\omega_{*pi} - \omega_{*pe})\hat{\omega}_{ki}$ and $\hat{\omega}_{Be} - \beta_e(\omega_{*pi} - \omega_{*pe}) = \hat{\omega}_{ke}$. Eqs. (42) and (43) describe kinetic ballooning mode and retain the leading order effects of trapped electron density fraction, finite ion Larmor radii ($b_i = k_{\perp}^2 T_i / m_i \omega_{ci}^2 < 1$), small magnetic drift frequency ($\omega_d / \omega < 1$) and small plasma β ($\beta < 1$). Making use of Eq. (42), Eq. (43) can be re-written as

$$\begin{aligned} \mathbf{B} \cdot \nabla \left(\frac{k_{\perp}^2}{B^2} \mathbf{B} \cdot \nabla (\Phi - \Psi) \right) + \beta \left(\frac{\mathbf{B} \times \nabla \ln P \cdot \mathbf{k}}{B} \right) \left(\frac{\mathbf{B} \times \boldsymbol{\kappa} \cdot \mathbf{k}}{B} \right) (\Phi - \Psi) + \frac{k_{\perp}^2}{V_A^2} \omega (\omega - \omega_{*pi}) \Phi \\ + R_1 \frac{m_i \omega_{ci}^2}{T_i V_A^2} \left\{ \left[(\omega_{*pi} - \omega_{*pe}) - \frac{(\omega - \omega_{*pe})}{4} \right] \hat{\omega}_{ke} \frac{(\omega - \omega_{*pi})}{(\omega - \omega_{*e})} \left(b_i - \frac{\hat{\omega}_{ki}}{\omega} \right) \right. \\ \left. - \frac{3}{2} \left(1 - \frac{\omega_{*pi}}{\omega} \right) \frac{(\omega - \omega_{*pe})}{(\omega - \omega_{*e})} \left[\hat{\omega}_{ki} \langle \hat{\omega}_{de} \rangle + \frac{\beta_2}{2} \hat{\omega}_{ki} (\omega_{*pe} - \omega_{*pi}) \right] \right. \\ \left. + \frac{15}{8} \left(1 - \frac{(1 + 2\eta_e)\omega_{*e}}{\omega} \right) \left[\hat{\omega}_{ki} \langle \hat{\omega}_{de} \rangle + \frac{\beta_e}{2} \hat{\omega}_{Bi} (\omega_{*pe} - \omega_{*pi}) \right] \right\} \Phi \simeq 0, \end{aligned} \quad (44)$$

where we have made use of $(\omega_{*i} - \omega_{*pe}) \hat{\omega}_{ki} = (V_A^2 T_i / m_i \omega_{ci}^2) \beta (\mathbf{B} \times \nabla \ln P \cdot \mathbf{k}) (\mathbf{B} \times \boldsymbol{\kappa} \cdot \mathbf{k}) / B^2$. Equation (44) provides the analytical understanding of the KBM stability property. It is clear that the first two terms of Eq. (44) are essentially the ideal MHD contribution with the first term representing the stabilizing field line bending term and the second term representing the instability drive if the pressure gradient is in the same direction as the field line curvature. The third term represents the ion inertia effect modified by the finite ion

Larmor radius effect in the ion diamagnetic drift frequency. The fourth term is proportional to the trapped electron density fraction and represents the kinetic contributions from the trapped electron density fraction as well as effects due to ion Larmor radii, particle gradient B and curvature drifts as well as density and temperature gradient drifts.

From our previous works [2,3] and the numerical solutions presented below we realize that at marginal stability the frequency of the kinetic ballooning mode (KBM) is given by $\omega = \omega_{*i}$ for $\eta_i = 0$ and $\omega > \omega_{*pi} \equiv (1 + \epsilon a_i)\omega_{*i}$ for $\eta_i \neq 0$. For $\eta_i = 0$, at marginal stability $\omega = \omega_{*i}$, the third term and the first and second terms in the curly bracket of the fourth term vanish. Thus, without the trapped electron density fraction, Eq. (44) is essentially the ideal MHD equation and the critical β of KBMs is identical to the ideal MHD critical β even though the other kinetic effects reduce the growth rate from the ideal MHD case [2,3]. With a finite trapped electron density fraction, the coefficient of the fourth term in Eq. (44) is negative and thus the trapped electron effect gives a stabilizing effect with the critical β increased (decreased) by a factor proportional to $O(\sqrt{\epsilon})$ for the first (second) stability as the numerical results show in Fig. 1.

For $\eta_i \neq 0$, we realize from the numerical solutions that at the marginal stability $\omega > \omega_{*pi}$. Then, the coefficient of third term in Eq. (44) is positive. Thus, in the absence of trapped electrons, the kinetic effect due to the third term is destabilizing and the critical β for the first stability is reduced from the ideal MHD critical β , which is verified by the numerical solutions presented in Figure 6 of Ref. [2]. The coefficient of the fourth term in Eq. (44) consists of three terms; the first and third terms are negative, but the second term is positive. However, the second term is smaller than the third term and the coefficient of the fourth term in Eq. (44) is negative, and thus, the trapped electron effect is stabilizing.

Next, we consider the small aspect ratio limit, $n_{eu}/n_e \equiv 1 - R_1 \sim O(B/2B_{max}) \ll 1$, then $R_2 \simeq 2/3 + O(B/2B_{max})^2$, and $R_3 \simeq 8/15 + O(B/2B_{max})^2$. Then, Eqn. (45) becomes

$$\frac{T_e}{q_e B} \delta B_{\parallel} = \frac{\beta_e}{2} \left(\frac{\omega_{*pe} - \omega_{*pi}}{\omega} \right) \quad (45)$$

and substituting this expression into Eqn. (36) and Eqn. (38) we obtain

$$\begin{aligned} \frac{n_{eu}}{n_e} \left(1 - \frac{\omega_{*e}}{\omega}\right) \Psi = & \left[\frac{q_i T_e}{q_e T_i} \left(1 - \frac{\omega_{*pi}}{\omega}\right) \left(b_i - \frac{\hat{\omega}_{Bi} + \hat{\omega}_{ki}}{2\omega}\right) \right. \\ & \left. + \frac{3}{2} \left(1 - \frac{\omega_{*pe}}{\omega}\right) \frac{\langle \hat{\omega}_{de} \rangle}{\omega} - \frac{\beta_e}{2} \left(\frac{\omega_{*pi} - \omega_{*pe}}{\omega}\right)^2 \right] \Phi, \end{aligned} \quad (46)$$

and

$$\begin{aligned} \mathbf{B} \cdot \nabla \left(\frac{k_{\perp}^2}{B^2} \mathbf{B} \cdot \nabla (\Phi - \Psi) \right) + \omega (\omega - \omega_{*pi}) \frac{k_{\perp}^2}{V_A^2} \Phi \\ + \beta \left(\frac{\mathbf{B} \times \nabla \ln P \cdot \mathbf{k}}{B} \right) \left(\frac{\mathbf{B} \times \boldsymbol{\kappa} \cdot \mathbf{k}}{B} \right) \Phi = 0. \end{aligned} \quad (47)$$

Note that Eq. (47) differs from the ideal MHD ballooning mode equation by the parallel electric field potential Ψ term in the field line bending term. Because the coefficient of the Φ term in Eq. (46) is negative, thus the Ψ term in Eq. (47) enhances the stabilizing field line bending effect. From Eq. (46) the parallel electric field arises from the difference between ions and trapped electron in their perpendicular motion (finite ion Larmor radius effect, ion magnetic drift, trapped electron perpendicular drift, and the response due to compressional magnetic field perturbation. Moreover, the parallel electric field is enhanced by $n_e/n_{eu} \gg 1$.

Equations (46) and (47) can be combined to give

$$\mathbf{B} \cdot \nabla \left(\frac{k_{\perp}^2}{B^2} \mathbf{B} \cdot \nabla S_c \Phi \right) + \frac{\omega(\omega - \omega_{*pi})}{V_A^2} k_{\perp}^2 \Phi + \beta \left(\frac{\mathbf{B} \times \boldsymbol{\kappa} \cdot \mathbf{k}_{\perp}}{B} \right) \left(\frac{\mathbf{B} \times \nabla P \cdot \mathbf{k}_{\perp}}{BP} \right) \Phi \simeq 0, \quad (48)$$

where

$$\begin{aligned} S_c = 1 + \frac{n_e}{n_{eu}} \left[\frac{\beta_e}{2} \left(\frac{\omega_{*pi} - \omega_{*pe}}{\omega}\right)^2 - \frac{q_i T_e}{q_e T_i} \left(\frac{\omega - \omega_{*pi}}{\omega - \omega_{*e}}\right) b_i \right. \\ \left. - \frac{3}{2} \left(\frac{\omega - \omega_{*pe}}{\omega - \omega_{*e}}\right) \frac{\langle \hat{\omega}_{de} \rangle}{\omega} + \left(\frac{\omega - \omega_{*pi}}{\omega - \omega_{*e}}\right) \frac{\hat{\omega}_{Be} + \hat{\omega}_{ke}}{2\omega} \right]. \end{aligned} \quad (49)$$

Note that the coefficient of n_e/n_{eu} in the above expression is positive and thus $S_c > 1$. For $n_e/n_{eu} \gg 1$ and $b_i \sim O(1)$ or $\beta \sim O(1)$, the n_e/n_{eu} term is much larger than unity, and $S_c \gg 1$. Physically, S_c is related to the perturbed parallel current, given by $\delta J_{\parallel} \simeq i \nabla_{\perp}^2 \nabla_{\parallel} (S_c \Phi) / \omega$, which gives rise to an enhanced stabilizing field line tension due to an enhanced parallel electric field ($-\nabla_{\parallel} \Psi$) resulting from the combined kinetic effects of trapped

electron dynamics and ion FLR and magnetic drift motion. The local dispersion relation is given by

$$\frac{\omega(\omega - \omega_{*pi})}{V_A^2} + \beta \left(\frac{\mathbf{B} \times \boldsymbol{\kappa} \cdot \mathbf{k}_\perp}{k_\perp B} \right) \left(\frac{\mathbf{B} \times \nabla \ln P \cdot \mathbf{k}_\perp}{k_\perp B} \right) \simeq S_c k_\parallel^2. \quad (50)$$

At marginal stability the critical beta for the KBM is given by

$$\beta_c \simeq S_c \beta_c^{MHD} - \frac{\omega(\omega - \omega_{*pi}) R_c L_p}{V_A^2}, \quad (51)$$

where $\beta_c^{MHD} = k_\parallel^2 R_c L_p$ is the ballooning instability threshold based on the ideal MHD theory, R_c is the radius of the magnetic field curvature and L_p is the pressure gradient scale length. For $\eta_i = 0$, $\omega = \omega_{*i}$ at the marginal stability. Then, the second term on the right hand side of Eq. (51) vanishes and $\beta_c = S_c \beta_c^{MHD}$ is enhanced over the ideal MHD threshold by S_c . For $\eta_i \neq 0$, $\omega > \omega_{*pi}$ at the marginal stability, thus $\omega(\omega - \omega_{*pi}) > 0$ and the second term on the right hand side of Eq. (51) reduces the β_c . However, S_c is also modified by the ω value at the marginal stability.

STABILITY ANALYSIS OF KINETIC BALLOONING MODES FOR ANALYTICAL ($\hat{s} - \alpha_p$) EQUILIBRIUM

More accurate solutions of KBMs must be carried out by performing numerical solutions of the eigenmode equations, Eqs. (36)-(38), which are a second order ordinary differential equation along the field line. Numerical studies of high- n (n is the toroidal mode number) KBMs based on Eqs. (36)-(38) have been performed for circular cross section tokamaks previously [2,3] by employing the ($\hat{s} - \alpha_p$) analytical model equilibrium where $\hat{s} = r q' / q$ is the magnetic shear, $\alpha_p = -2P' R_0 q^2 / B_0^2$, q is the safety factor, r is the minor radius, R_0 is the major radius, P is the plasma pressure, B_0 is the averaged magnetic field intensity over a flux surface. We adopt the high- n WKB-ballooning formalism, and to the lowest order in $(1/n)$ the radially local high- n eigenmode equation is obtained by choosing $S = n(q\theta - \zeta - \int \theta_k dq)$, where θ_k is to be determined from a higher order radially non-local analysis [8,9]. Based on

the $(\hat{s} - \alpha_p)$ equilibrium model for circular cross section tokamaks, we have $k_{\perp}^2 = k_{\theta}^2[1 + h(\theta)^2]$, $k_{\theta} = nq/r$, $h(\theta) = \hat{s}(\theta - \theta_k) - \alpha_p \sin\theta$, $\mathbf{B} \times \boldsymbol{\kappa} \cdot \nabla S = -(Bk_{\theta}/R_0)[\cos\theta + h(\theta)\sin\theta]$. In general we need to solve the radially local eigenmode equation for all θ_k in order to perform a two-dimensional eigenmode analysis. However, we shall choose $\theta_k = 0$ because the most unstable modes are usually related to $\theta_k = 0$.

We define the parameters $L_n = (d \ln n_i / dr)^{-1}$, $\varepsilon_n = L_n / R_0$, $\eta_e = d \ln T_e / d \ln n_e$, $\eta_i = d \ln T_i / d \ln n_i$, $\alpha_p = (q^2 / \varepsilon_n)[\beta_e(1 + \eta_e) + \beta_i(1 + \eta_i)]$, $\beta_e = 2n_e T_e / B^2$, $\beta_i = 2n_i T_i / B^2$, $\beta = \beta_e + \beta_i$, $b_{\theta} = k_{\theta}^2 \rho_i^2 / 2$, $\varepsilon = r / R_0$ is the inverse aspect ratio. Then, $\omega_{*pi} = (1 + \eta_i)\omega_{*i}$, and $\omega_{*pe} = (1 + \eta_e)\omega_{*e}$.

Figure 1 shows critical β_c values of the first and second stability boundaries for KBMs versus the inverse aspect ratio ε , which demonstrates the stabilizing effect of trapped electrons on β_c . The fixed parameters are $b_{\theta} = \varepsilon_n = 0.1$, $\hat{s} = 0.5$, $q = T_e / T_i = 1$, $\eta_e = \eta_i = 0$. It is clear that for small ε the increase in β_c from the $\varepsilon = 0$ case for the first stability boundary and the reduction in β_c from the $\varepsilon = 0$ case for the second stability boundary are proportional to $\sqrt{\varepsilon}$, which represents the trapped electron fraction.

The numerical results of the high- n eigenmode equations clearly confirm the qualitative results of the local solutions. A more complete eigenmode calculation including extensive kinetic effects based on numerical equilibria has also indicated that the kinetic ballooning mode will be stabilized in the small aspect ratio tokamaks [10]. However, the physical mechanism of the KBM stabilization was not specifically identified in these studies. Therefore, it would be worthwhile to carry out a more extensive calculation to address the kinetic effects of trapped electrons and finite ion Larmor radii in realistic NSTX equilibria or other low aspect ratio toroidal devices.

STABILITY ANALYSIS OF KINETIC BALLOONING MODES FOR NSTX EQUILIBRIUM

To study the stability of KBMs in NSTX numerical equilibria, we choose the baseline NSTX equilibrium parameters: major radius at the geometrical center is $R_0 = 0.86m$, minor radius of last magnetic surface is $a = 0.68m$, and the aspect ratio is $R_0/a = 1.27$, the last surface ellipticity is $\kappa = 1.63$ and triangularity is $\delta = 0.417$, the vacuum magnetic field at the geometrical axes $R = R_0$ is $B_0 = 0.3T$. To simplify the interpretation of the numerical solutions we chose constant temperature with $T_e = T_i = 1keV$ so that $\eta_i = \eta_e = 0$, which eliminates the temperature gradient driven modes. The central electron density is $n_{e0} = 2.9 \times 10^{13}cm^{-3}$, and the density profile is identical to the plasma beta profile. The beta at the magnetic axis is $\beta_0 \equiv 2P(0)/B_0^2 = 38\%$, and the volume-averaged beta is $2\langle P \rangle/B_0^2 = 9.075\%$. The q -profile is non-monotonic and has a region of negative shear inside of $q_{min} = q(r/a = 0.3) = 0.93$, where $r^2/a^2 \equiv \Psi_{tor}$, and Ψ_{tor} is the toroidal magnetic flux normalized to zero at the magnetic axis and unity at the plasma edge. The left figure in Figure 2 shows the radial profiles of plasma β and q , and the right figure in Figure 2 shows the nested magnetic flux surfaces of the NSTX equilibrium. The numerical NSTX equilibrium is computed using computationally efficient ESC code [11].

The high- n WKB-Ballooning kinetic equations, Eqs. (36)-(38), are solved by employing the HINST code [12] with $\theta_k = 0$. Figure 3 shows the dependence of the KBM growth rate and real frequency (normalized by $\omega_{A0} = V_A(0)/q(0)R_0$) on the minor radius r/a for the baseline NSTX equilibrium for $n = 12$. The KBM is unstable in the range of $0.4 > r/a > 0.28$, which is much smaller than the unstable region ($r/a < 0.45$) of the ideal MHD ballooning mode, whose growth rates are also shown in Figure 3. Note that at the marginal stability of the KBM, its real frequency equals the local ion diamagnetic drift frequency ω_{*i} , which is consistent with our previous studies [2,3], and the KBM growth rate is much smaller than the ideal MHD growth rate. Also, when the KBM is unstable, its real frequency is smaller than the local ω_{*i} , and the most unstable KBM occurs near $r/a = 0.33$.

Figure 4 shows the dependence of the KBM growth rate and frequency (normalized by ω_{A0}) on the plasma beta at $r/a = 0.35$ for $n = 12$. For each β value we compute a new equilibrium by varying the temperature, while keeping the other plasma profiles fixed. For unstable KBMs the real frequency is close to but below the local background ion diamagnetic drift frequency, ω_{*i} . The instability is stabilized by increasing beta. The KBM is stable for $\beta > 0.25$, which corresponds to equilibria with a central beta value of $\beta(0) = 0.5$. Note that at this critical point the mode frequency matches approximately the ion diamagnetic frequency, which is in agreement with our previous studies [2,3]. For $\beta \leq 0.05$ the magnetic shear is weak and the eigenmode solutions extend to a very large θ distance. It is thus difficult to identify the first stability boundary numerically.

Figure 5 shows the dependence of the complex KBM eigenfrequency (normalized by ω_{A0}) on the toroidal mode number n at $r/a = 0.35$ with a local $\beta \simeq 0.17$ for the baseline NSTX equilibrium. Note that the unstable n-spectrum is broad and the growth rate is reduced for higher n 's due to FLR effects.

Figure 6 shows the marginal stability boundary for the KBMs and the ideal MHD ballooning modes in the local β and r/a plane for $n = 12$. To compute the critical β values for each flux surface, we construct new equilibria by varying the central density value $n_e(0)$ (or $\beta(0)$) while keeping other equilibrium quantities fixed. For the baseline NSTX equilibrium the plasma beta is larger than the critical beta for unstable ideal MHD ballooning modes in a very broad region for $r/a < 0.46$ as shown in Fig. 6. However, the stability boundary for KBMs forms a closed curve and KBMs are stable in the region outside this closed curve. For the NSTX equilibrium KBMs are unstable from $r/a = 0.28$ to $r/a = 0.37$. Note that our HINST calculations do not find unstable KBMs up to $\beta(0) = 1$. Because the average beta for the NSTX equilibrium is $\langle\beta\rangle = 9.1\%$ and the experimentally achieved values are about a factor of three larger, we expect full stabilization of KBMs in high β NSTX discharges.

To study the aspect ratio effect, we perform stability calculations for an equilibrium with a slightly larger aspect ratio ($R_0/a = 1.67$) than that in the baseline NSTX case ($R_0/a = 1.27$). Other parameters are the same as in the baseline NSTX equilibrium. Figure 7

shows the marginal stability boundary for the ideal MHD ballooning modes and KBMs in the β and r/a plane for $n = 12$. For this equilibrium the ideal MHD ballooning modes are unstable for $r/a < 0.5$ and there is no second stability boundary in this case, However, for KBMs there is a second stability boundary for $0.28 > r/a > 0.18$. Note that for this equilibrium KBMs are unstable in a larger radial domain ($0.28 < r/a < 0.44$) mainly because it requires larger minor radii for the stabilizing trapped electron effect to become effective in a larger aspect ratio device. For KBMs the stabilizing effect comes from the larger number of trapped electrons above $r/a = 0.4$. For $r/a < 0.3$ the KBMs are stabilized due to weakly negative shear and and stronger FLR stabilization, where $k_{\perp} \sim 1/r$ is large near the magnetic axis. It is important to note again that the most unstable region is near the zero shear surface at $r/a \simeq 0.3$.

To study more realistic plasma profiles, we introduce the plasma temperature gradient effect for the baseline NSTX equilibrium presented in Fig. 2 by choosing both the electron and ion temperature profiles to be the same as the density profile so that $\eta_e = \eta_i = 1$ for all minor radii. Note that the density profile is proportional to the square root of the pressure profile and is different from that in the constant temperature case presented in Figures 3-6. Figure 8 shows the KBM frequency and growth rate, and ion diamagnetic drift frequency (normalized by ω_{A0}) versus r/a for $n = 12$. Note that the real frequency of the KBM is larger than $(1 + \eta_i)\omega_{*i}$. Figure 9 shows the critical betas for the KBM and the ideal MHD ballooning mode. For the chosen temperature gradient values KBMs are unstable in the domain bounded by the β_{crKBM} curve. Near the q_{min} location ($r/a \simeq 0.3$) the first stability critical beta is larger than the zero temperature gradient case presented in Fig 6. It is clear that the temperature gradients make KBMs more unstable and the second stability critical beta is much larger than the zero temperature gradient case. For the specific NSTX pressure profile KBMs are unstable in the radial range $0.35 > r/a > 0.27$ and there seems to have no second stability.

SUMMARY AND DISCUSSION

In this paper we have identified a physical process of stabilizing the ballooning instability in collisionless tokamak plasmas by the combined kinetic effects of trapped electron dynamics and the difference in the motion perpendicular to the ambient magnetic field between electrons and ions due to finite ion Larmor radii and magnetic drift. For large aspect ratio $r/R_0 \ll 1$, the first stability β threshold for exciting KBMs is increased and the second stability β threshold is reduced in comparison with the ideal MHD ballooning mode β_c by a factor proportional to $\sqrt{r/R_0}$. The unstable β region is much reduced because the kinetic effects give rise to a large parallel electric field and hence a parallel current that enhances the stabilizing effect of field line tension. For small aspect ratio $r/R_0 \sim 1$, the KBM β_c is enhanced over the ideal MHD threshold by a factor proportional to n_e/n_{eu} . For $R_0/r = 1.5$, $n_e/n_{eu} \simeq 10$ and we expect the KBM to be stable except in the very weak shear region. Numerical solutions for the low aspect ratio, baseline NSTX equilibrium with a weak reverse shear support this stabilizing kinetic effects for the KBM. For the baseline NSTX equilibrium the KBM is expected to be stable in most the radial region except in the weak magnetic shear region near q_{min} . However, in the unstable region the KBM growth rate is very weak and is much smaller than the ideal MHD ballooning mode growth rate by more than a factor of 10.

ACKNOWLEDGMENT

This work was supported by US DoE contract DE-AC02-76-CHO-3073.

-
- [1] Catto, P. J., W. M. Tang, and D. E. Baldwin, *Plasma Phys.*, *23*, 639 (1981).
- [2] Cheng, C. Z., *Phys. Fluids*, *25*, 1020 (1982).
- [3] Cheng, C. Z., *Nucl. Fusion*, *22*, 773 (1982).
- [4] Cheng, C. Z., *J. Geophys. Res.*, *96*, 21159 (1991).
- [5] Cheng, C. Z., and Q. Qian, *J. Geophys. Res.*, *99*, 11193 (1994).
- [6] Cheng, C. Z., N. N. Gorelenkov, and C. T. Hsu, *Nucl. Fusion*, *35*, 1639 (1995).
- [7] Cheng, C. Z., and J. R. Johnson, *J. Geophys. Res.*, *104*, 413 (1999).
- [8] Connor, J. W., et al., *Proc. R. Soc. London A*, *365*, 1 (1979).
- [9] Dewar, R. L., et al., *Nucl. Fusion*, *21*, 1493 (1981).
- [10] Rewoldt, G., W. M. Tang, S. Kaye, and J. Menard, *Phys. Plasmas*, *3*, 1667 (1996).
- [11] L. E. Zakharov and A. Pletzer, *Phys. Plasmas*, *6*, 4693 (1999).
- [12] N. N. Gorelenkov, C. Z. Cheng, W. Tang, *Phys. Plasmas*, *5*, 3389 (1998).
- [13] Cheng, C. Z. and A. T. Y. Lui, *Geophys. Res. Lett.*, *25*, 4091 (1998).

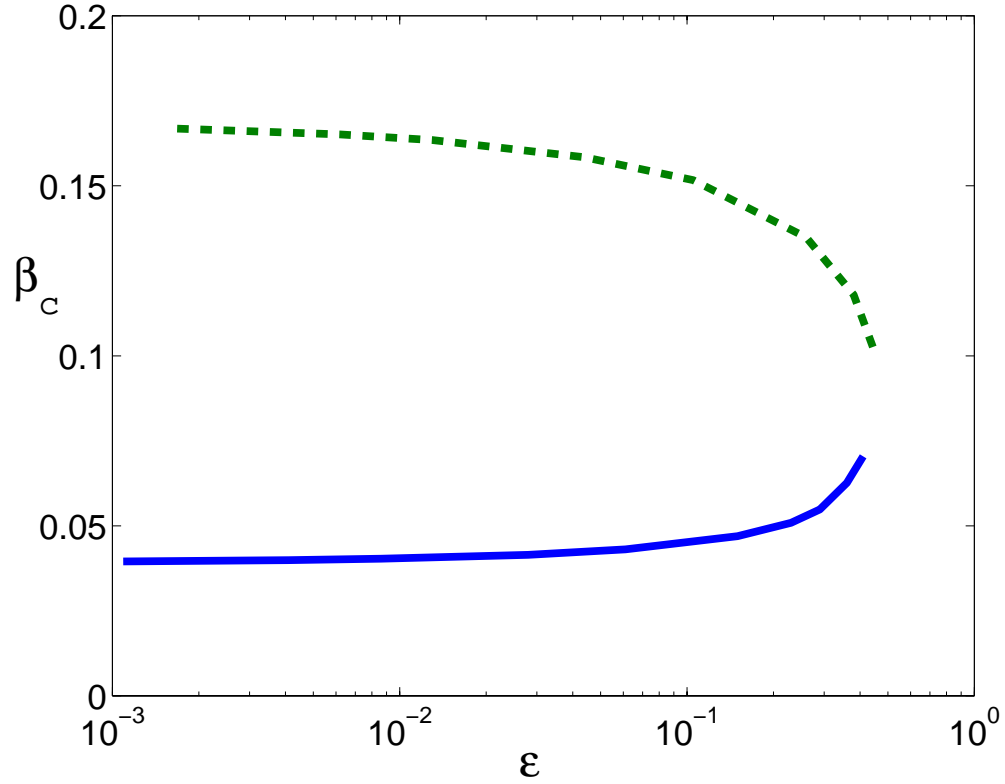


FIG. 1. Critical betas of the first and second stability of the kinetic ballooning mode versus the inverse aspect ratio $\epsilon = r/R_0$ for a large aspect ratio ($\hat{s} - \alpha_p$) equilibrium. The fixed parameters are $b_\theta = 0.1$, $\epsilon_n = 0.1$, $\hat{s} = 0.5$, $q = 1$, $\eta_e = \eta_i = 0$, $T_e/T_i = 1$.

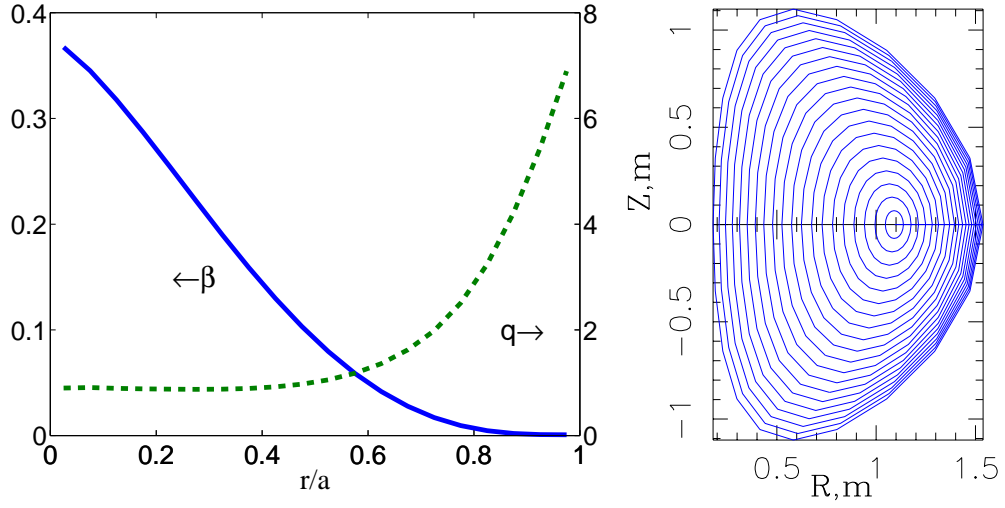


FIG. 2. (a) β and q profiles as functions of r/a , which is the square root of the normalized toroidal flux of the baseline NSTX equilibrium, and (b) the nested magnetic surfaces.

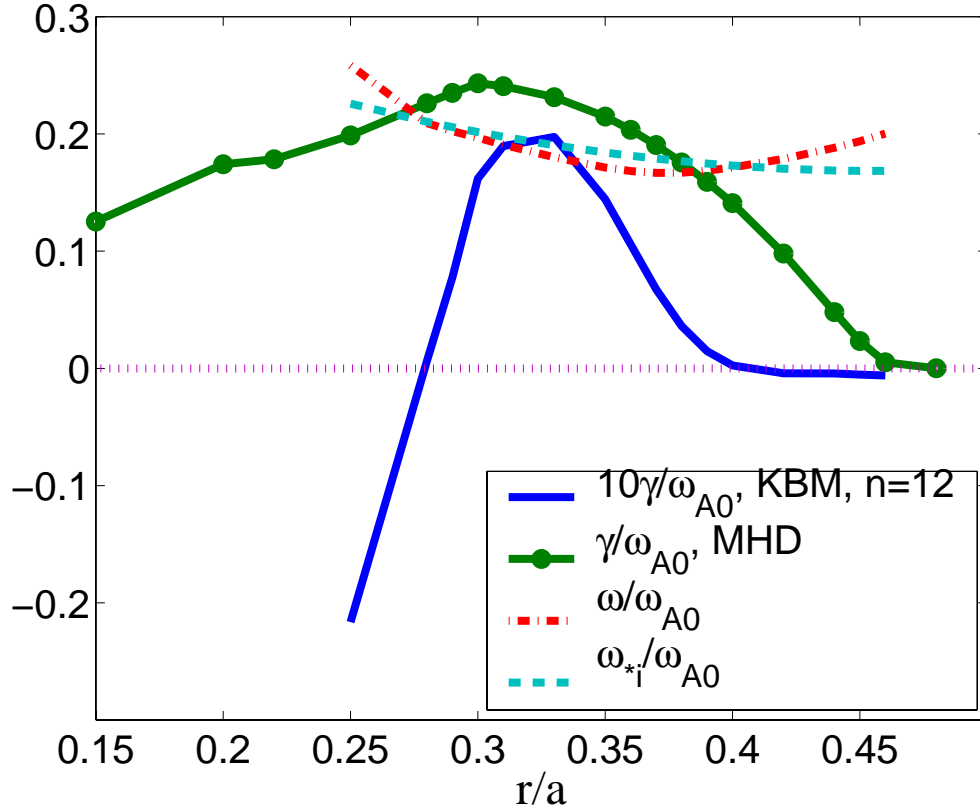


FIG. 3. The kinetic ballooning mode frequency and growth rate (normalized by $\omega_{A0} = V_A(0)/q(0)R_0$) versus the minor radius for $n = 12$ for the baseline NSTX equilibrium. Also shown are the MHD ballooning mode growth rate and ion diamagnetic drift frequency.

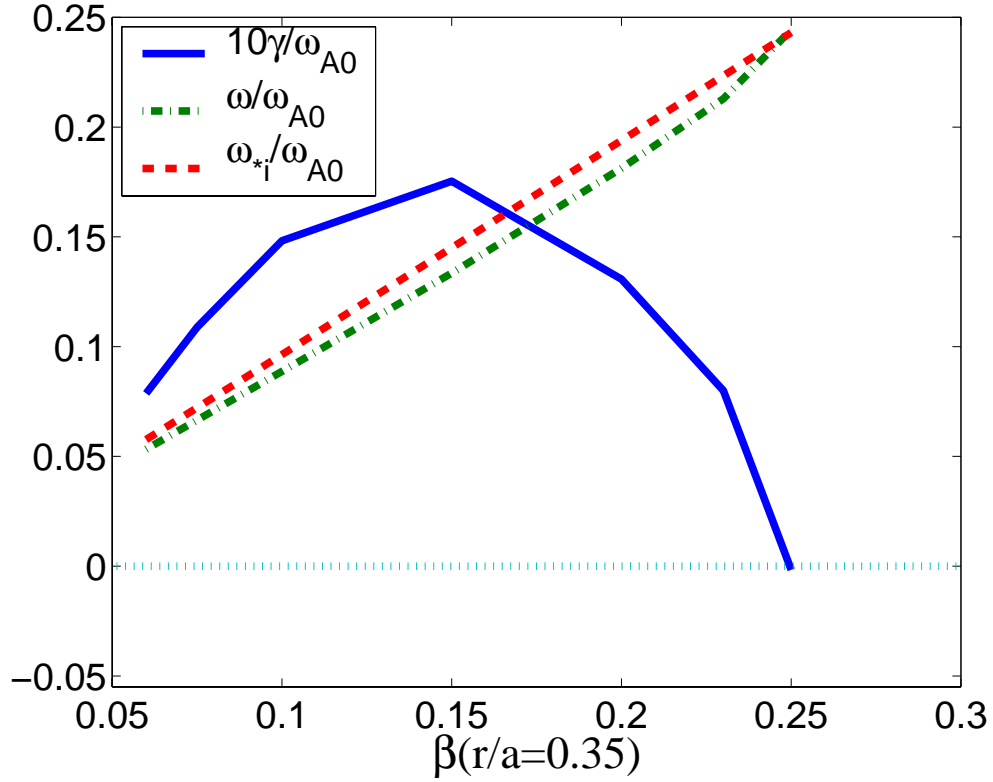


FIG. 4. The kinetic ballooning mode frequency and growth rate (normalized by $\omega_{A0} = V_A(0)/q(0)R_0$) versus the plasma β value at $r/a = 0.35$ for the $n = 12$ modes. ω_{*i} is also shown.

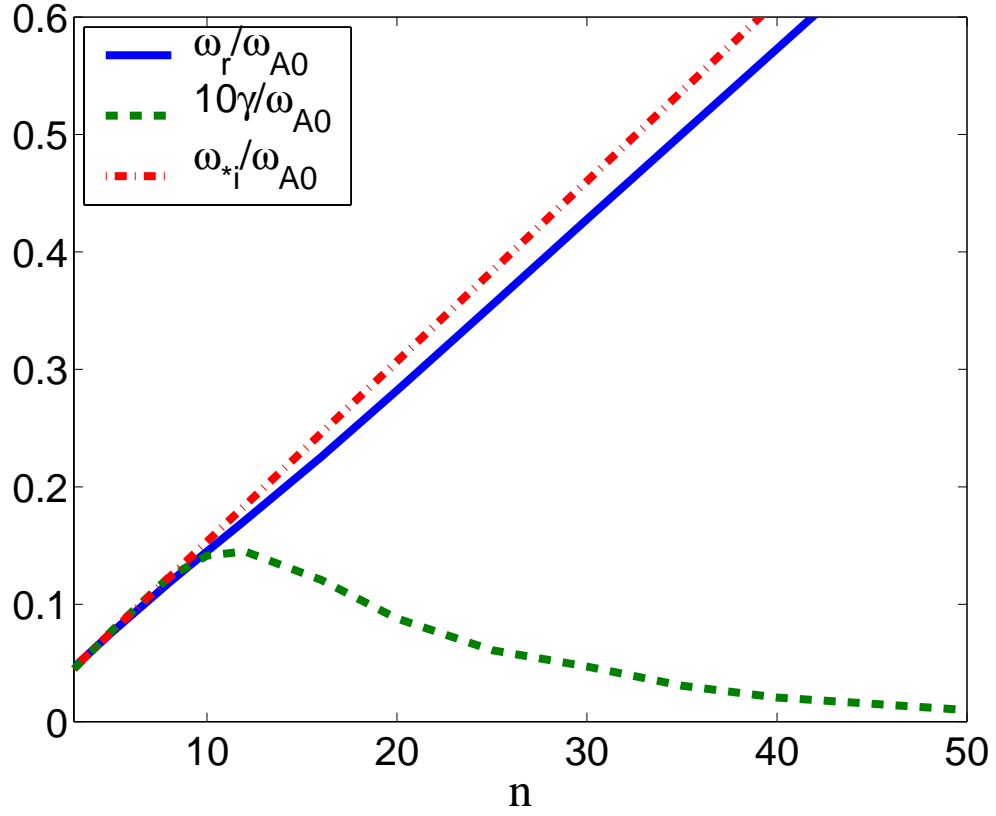


FIG. 5. The kinetic ballooning mode frequency and growth rate, and ion diamagnetic drift frequency (normalized by $\omega_{A0} = V_A(0)/q(0)R_0$) versus the toroidal mode number at $r/a = 0.35$ and with local $\beta \simeq 0.17$ for the baseline NSTX equilibrium.

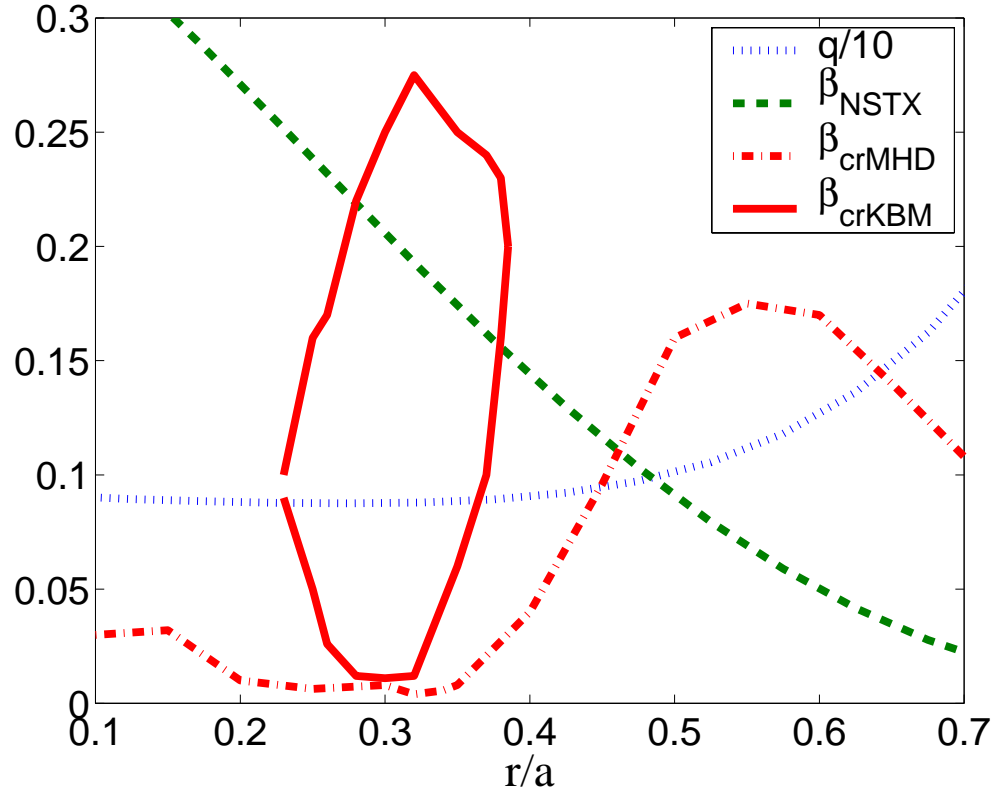


FIG. 6. The critical beta for the $n = 12$ kinetic ballooning mode and the ideal MHD ballooning mode for the baseline NSTX equilibria with aspect ratio $R_0/a = 1.27$. Also shown are the NSTX β and q profiles.

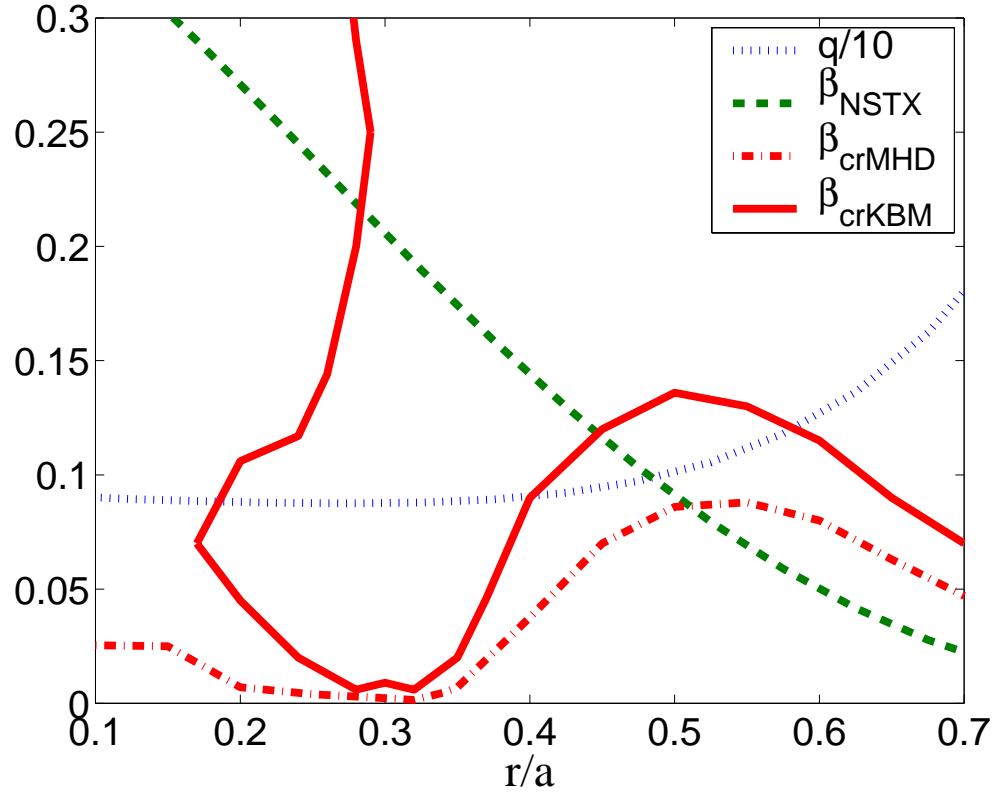


FIG. 7. The critical beta for the $n = 12$ kinetic ballooning mode and the ideal MHD ballooning mode for an NSTX equilibrium with a larger aspect ratio $R_0/a = 1.67$ than the baseline NSTX equilibrium. Also shown are the NSTX β and q profiles.

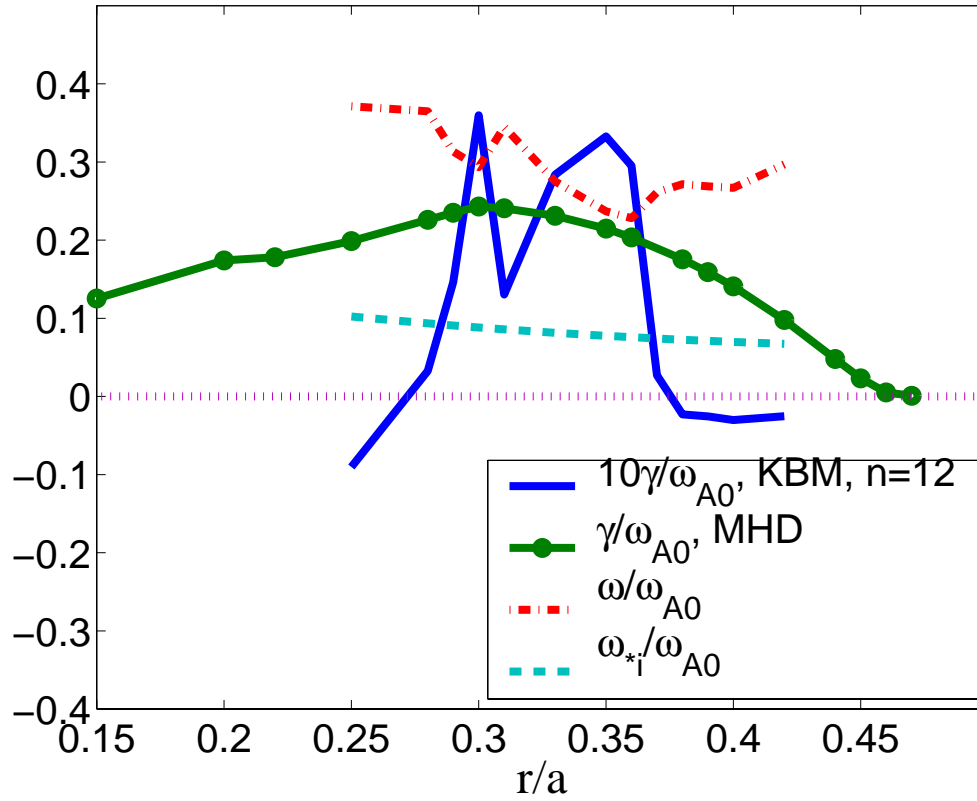


FIG. 8. The kinetic ballooning mode frequency and growth rate, and ion diamagnetic drift frequency (normalized by $\omega_{A0} = V_A(0)/q(0)R_0$) versus r/a for $n = 12$ and $\eta_e = \eta_i = 1$ for the baseline NSTX equilibrium.

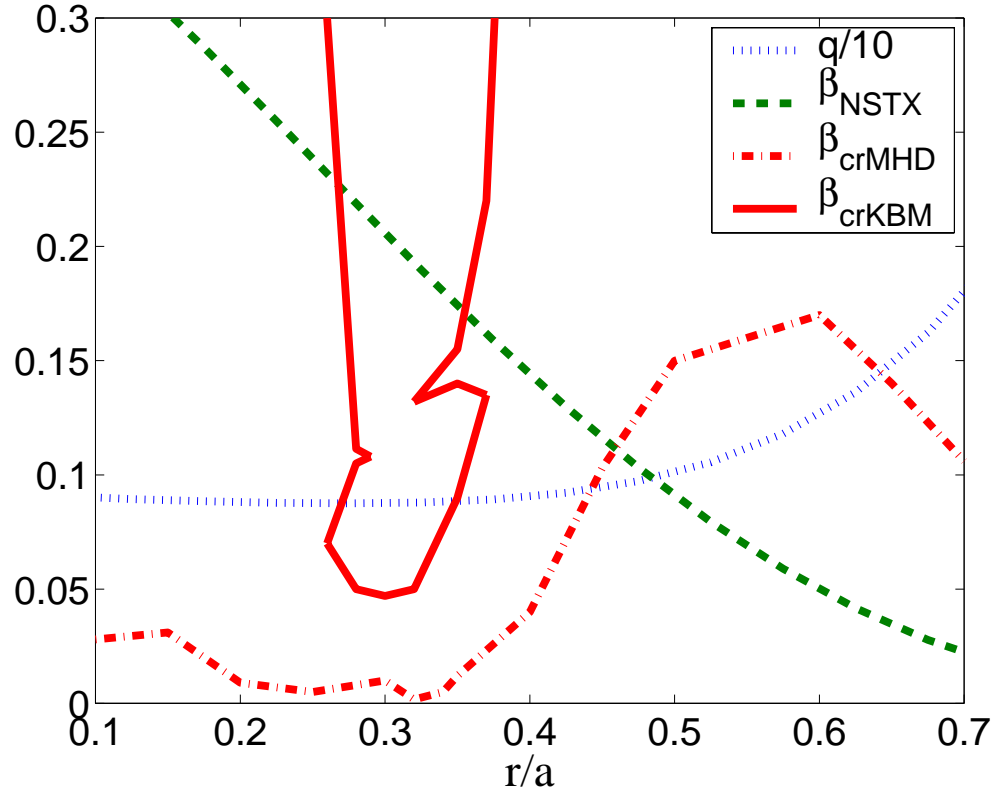


FIG. 9. The critical beta for the kinetic ballooning mode and the ideal MHD ballooning mode for the baseline NSTX equilibria with $R/a = 1.27$ and $\eta_e = \eta_i = 1$ for the $n = 12$ mode. Also shown are the NSTX β and q profiles.

External Distribution

Plasma Research Laboratory, Australian National University, Australia
Professor I.R. Jones, Flinders University, Australia
Professor João Canalle, Instituto de Fisica DEQ/IF - UERJ, Brazil
Mr. Gerson O. Ludwig, Instituto Nacional de Pesquisas, Brazil
Dr. P.H. Sakanaka, Instituto Fisica, Brazil
The Librarian, Culham Laboratory, England
Mrs. S.A. Hutchinson, JET Library, England
Professor M.N. Bussac, Ecole Polytechnique, France
Librarian, Max-Planck-Institut für Plasmaphysik, Germany
Jolan Moldvai, Reports Library, Hungarian Academy of Sciences, Central Research Institute
for Physics, Hungary
Dr. P. Kaw, Institute for Plasma Research, India
Ms. P.J. Pathak, Librarian, Institute for Plasma Research, India
Ms. Clelia De Palo, Associazione EURATOM-ENEA, Italy
Dr. G. Grosso, Instituto di Fisica del Plasma, Italy
Librarian, Naka Fusion Research Establishment, JAERI, Japan
Library, Laboratory for Complex Energy Processes, Institute for Advanced Study,
Kyoto University, Japan
Research Information Center, National Institute for Fusion Science, Japan
Dr. O. Mitarai, Kyushu Tokai University, Japan
Dr. Jiengang Li, Institute of Plasma Physics, Chinese Academy of Sciences,
People's Republic of China
Professor Yuping Huo, School of Physical Science and Technology, People's Republic of China
Library, Academia Sinica, Institute of Plasma Physics, People's Republic of China
Librarian, Institute of Physics, Chinese Academy of Sciences, People's Republic of China
Dr. S. Mirnov, TRINITI, Troitsk, Russian Federation, Russia
Dr. V.S. Strelkov, Kurchatov Institute, Russian Federation, Russia
Professor Peter Lukac, Katedra Fyziky Plazmy MFF UK, Mlynska dolina F-2,
Komenskeho Univerzita, SK-842 15 Bratislava, Slovakia
Dr. G.S. Lee, Korea Basic Science Institute, South Korea
Institute for Plasma Research, University of Maryland, USA
Librarian, Fusion Energy Division, Oak Ridge National Laboratory, USA
Librarian, Institute of Fusion Studies, University of Texas, USA
Librarian, Magnetic Fusion Program, Lawrence Livermore National Laboratory, USA
Library, General Atomics, USA
Plasma Physics Group, Fusion Energy Research Program, University of California
at San Diego, USA
Plasma Physics Library, Columbia University, USA
Alkesh Punjabi, Center for Fusion Research and Training, Hampton University, USA
Dr. W.M. Stacey, Fusion Research Center, Georgia Institute of Technology, USA
Dr. John Willis, U.S. Department of Energy, Office of Fusion Energy Sciences, USA
Mr. Paul H. Wright, Indianapolis, Indiana, USA

The Princeton Plasma Physics Laboratory is operated
by Princeton University under contract
with the U.S. Department of Energy.

Information Services
Princeton Plasma Physics Laboratory
P.O. Box 451
Princeton, NJ 08543

Phone: 609-243-2750
Fax: 609-243-2751
e-mail: pppl_info@pppl.gov
Internet Address: <http://www.pppl.gov>